

The Development of a MOA Leakage Current Tester Based On Floating-point DSP

Norbert. C. Cheung

Department of Electrical Engineering
Hong Kong Polytechnic University
Hungghom, Kowloon, Hong Kong
eencheun@polyu.edu.hk

Fei Li

Department of Electrical Engineering
Xian Jiaotong University
Xian, China

Abstract

In this paper the development of a tester for the leakage current of MOA (Metal Oxide Arrester) based on floating-point DSP is introduced and the working principle of the tester is described. Utilizing the powerful calculation performance of DSP TMS320C32, the software algorithm of digital filtering, interpolation method and correlation processing is implemented. The experiments have proved that the tester is accurate and stable, and that the tester shows good performances and strong ability to resist interference.

Key words:

DSP, Leakage Current, Metal Oxide Arrester, Digital filtering

1. Introduction

Lighting Arrester is one of the important protective equipment to guarantee the safe operation of power systems. Its protection function will play an important role to guaranteeing the safety operation of power supply systems. Currently, two types of arrester are being used in China; they are the valve type arresters and metal oxide arresters (MOA). MOA is more widely used, because of its highly nonlinear electrical characteristics.

In the case of AC operation, the total leakage current of MOA is the sum of capacitive and resistive components. At the normal circumstances, the leakage current is mainly capacitive; resistive component only occupies a small part, about 10% - 20%. Due to aging, environmental contamination and inner insulating components damaged, the resistive current will increase substantially. However, the capacitive current will have little change. The increase of the resistive component will lead to the heating up of the arrester, which may finally cause the damage of the device. Sometimes, an explosion may occur. Therefore, the resistive component is of great importance to the MOA and it should be monitoring continuously [Akbar and Ahamd, 1999].

The MOA leakage current tester proposed in this paper is to address the above problem. It uses 32-bit floating point DSP as the control kernel and the data processing unit. All signal processing units, e.g. digital filtering, correlation analysis and interpolation method are programmed in software. The tester can operate with

live line connected, thus making the continuous monitoring of the MOA possible. It gives early warnings to the operator to avoid the loss caused by explosion and ensure the system's safe operating.

2. The Measurement Principle

The inherit nonlinearity nature of the MOA is suitable for clamping the voltage to an acceptable level so as to protect the power transporting circuit when a high voltage surge comes to transmission equipment due to switching operations and lightning. The electrical properties of a MOA in the leakage current range can be represented by the simplified model shown in Fig. 1 [Lundquist J. et al., 1990].

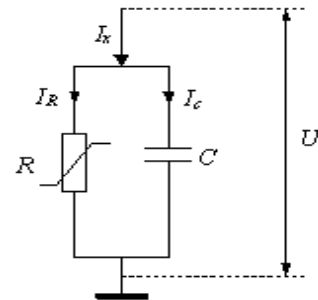


Fig.1 Electrical representation of a MOA

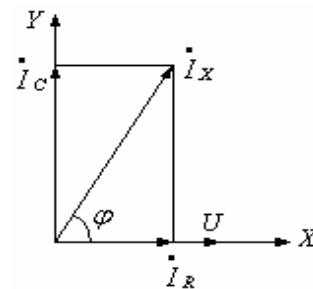


Fig.2 Relation of current vectors

The total leakage current is the sum of the capacitive and resistive components. Their vector relation is shown in Fig. 2. The equations of current vectors can be expressed as follows:

$$\dot{I}_R = \dot{I}_X * \cos\varphi \quad (1)$$

$$\dot{I}_C = \dot{I}_X * \sin\varphi \quad (2)$$

As long as the total leakage current value \dot{I}_X and the phase angle deviation φ in the metering equations can be obtained, the resistive component of the leakage

I_R can be derived. Furthermore, through the analysis of I_R , the MOA's operation condition can be judged.

2 Realization of the MOA Tester Hardware

A floating DSP, TMS320C32, forms the kernel unit of the tester. It is a high-performance, 32-bit floating point device and it can execute up to 30 million floating-point operations per second (MFLOPS). It has Bootstrap loader that can load program from low-speed-low-cost EPROM to off-chip fast-speed SRAM during power up.

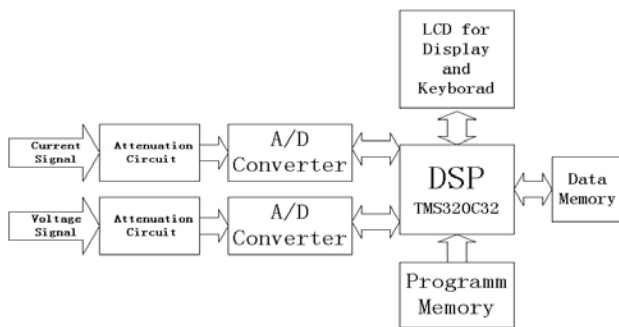


Fig. 3 Block diagram of the tester

The block diagram of the MOA leakage current tester is shown in Fig. 3. In the forepart, isolated current sensors and position transformers (PT) are used to fetch the leakage current signal and voltage signal of PT's second side. Fig.4 shows how the field signals are acquired into the tester. In the field, the leakage current of the MOA is obtained by the current transformer through shorting the lighting counter installed in the grounding lead of MOA.

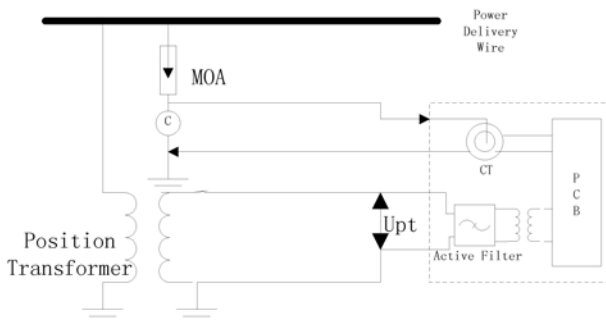


Fig.4 Acquiring the field signals

After the attenuation circuits, the signals are fed into the ADC directly. The digital signals are presented as 12-bit binary code and are processed by the DSP chip. An LCD module displays the results: these include the total leakage current, the resistive component, the voltage of power system and the angle deviation φ between voltage and leakage current. All processes, including sampling, keyboard control, LCD displaying and data computing are controlled by the DSP.

The A/D converter has a sampling speed of 500kbps at 12-bit resolution. At the beginning of the measurement, two ADC samples of the voltage and current signals are stored into the RAM. Sampling is stopped after sampling 10 cycles of signals. Then the data are processed by DSP. The synchronous sampling method can decrease the phase error from asynchronous sampling.

3 Software Algorithm

3.1 Analysis of Voltage Waveforms

The tester measures leakage current produced in MOA by voltage of power system so that the quality of voltage of power system directly influences the precision of measure results of the tester, and the voltage quality in power network can directly determine the software algorithm adopted in this system.

Quality of voltage of the power system is influenced by three factors: voltage fluctuation of the power system [Sun S.Q., 1998], frequency fluctuation of power system [Cai B., 1998] and interference of harmonic waves of the power system [Xu K.M. et al., 1991]. Voltage fluctuation is mainly caused by fluctuant loads, which changes irregularly. Frequency fluctuation is caused by using excessive passive power devices being used in power system. Because of frequency fluctuation, the practical frequency of power system does not always equal to 50 Hz. Based on the regulations by the ministry of Electric Power, the frequency deviation of fundamental wave of voltage of power system is limited to below 0.5 Hz. In the nonlinear loads of power systems, the harmonic waves mainly consist of 3rd harmonic component and 5th harmonic component. Sometimes the ratio of virtual value of third and fifth harmonic components to primary wave can be up to 20%, and cause severe distortion to the original wave.

3.2 Digital Filtering

In the design, an FIR digital filter is used to eliminate the interference of high harmonic waves and high frequency electromagnetic waves. The digital filtering is realized by the convolution of two series of discrete data, that is, digital filter data series convolutes with sampled signal data series so as to eliminate the noise signals for obtaining useful signals. FIR filter can bring about phase delay, but what this delay does not affect the operation of the tester. The tester needs to seek is the phase angle difference between the current and the voltage; the FIR filter has the same phase delay to the current and voltage signals so that the phase delay caused by FIR would not affect the accuracy of this design.

A 1024-order Hamming low-pass digital filter is used. The Hamming window method provides some

advantages: Its energy leakage is low and its stop-band is restrained. Therefore the frequency characteristic of Hamming window fluctuates very little. The frequency characters of the digital filter designed are shown in Fig.5. The cut-off frequency is 60 hertz.

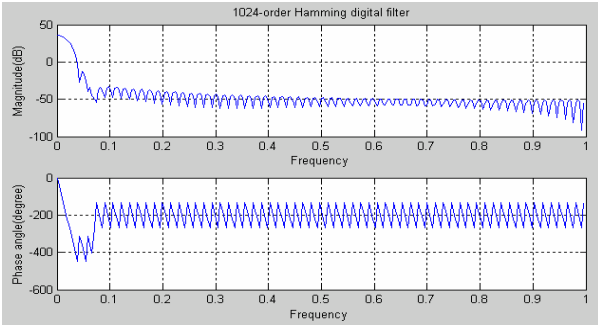


Fig.5 Magnitude and Phase response of the Hamming window

Fig.6 shows the effect of the Hamming digital filter. After processing filtering, 3rd harmonic, 5th harmonic and high frequency electromagnetic interference in the sampled sequence are eliminated.

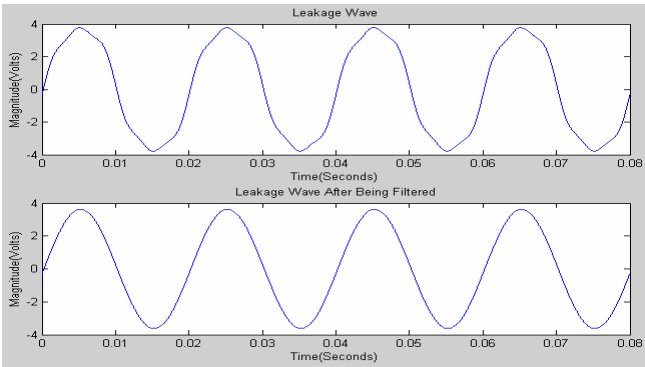


Fig.6 Effect of 1024-order Hamming digital filter

3.3 Period Measurement & Interpolate Algorithm

Owing to the real-life conditions, the frequency of voltage in power grid can fluctuate so much that it is necessary for us to obtain the actual cycle of signals via calculation. After the signals are treated via the digital filter, the actual signal cycles can be obtained via the Zero Crossing Technique in software.

In the design, signal wave sampling per cycle is 4096 points with sampling frequency $f_s = 50\text{Hz} * 4096$ (i.e. 204.8kHz), and sampling time interval is $\Delta t = \frac{1}{f_s}$. Supposing the actual signals with actual frequency f are:

$$y(t) = A * \sin(2\pi ft + \phi) \quad (3)$$

where A : the amplitude
 ϕ : the phase angle

Thus, the maximum varying amplitude of signals within the sampling time interval is :

$$\Delta y(t)_{\max} = y(t)'_{\max} * \Delta t = 2\pi A f \Delta t \quad (4)$$

According to (4), the zero crossing points of signal wave can be obtained by testing whether the dates in series are in the range $[-\Delta y(t)_{\max}, \Delta y(t)_{\max}]$ when $f = 50.5\text{Hz}$. If there is more than a zero crossing point in the range, the Least Square Method is used to calculate one zero crossing point. As the zero crossing point is obtained, the period of signal wave can be derived.

After obtaining the signal cycle, a linear interpolation method was used with a frequency of 1024-times of signal frequency f obtained by the Zero Crossing Technique.

The linear interpolation used in software is presented in detail as follows:

Letting x_n be the sampling sequence that has been filtered and the corresponding sampling time sequence

is $t_x(n) = \frac{n}{f_s}$ between each point. After interpolation, sequence y_n , which includes 1024 points per period of signal wave, is obtained. Let f be the real frequency obtained by Zero Crossing Technique. Then corresponding interpolation time sequence is

$$t_y(n) = \frac{n}{1024 * f}$$

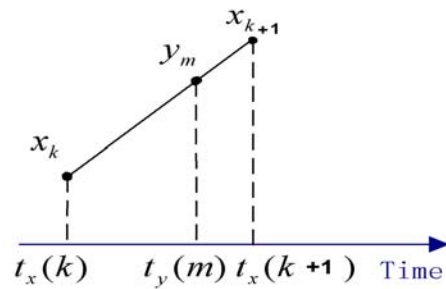


Fig.7 Principle of Linear Interpolation Method

According to Fig.7, the equation of interpolation is given:

$$y_m = x_{k+1} - \frac{t_x(k+1) - t_x(k)}{\Delta t_x} (x_{k+1} - x_k) \quad (5)$$

where

$$t_x(k) < t_y(m) < t_x(k+1),$$

$$\Delta t_x = t_x(k+1) - t_x(k) = \frac{1}{f_s}$$

3.4 Correlation Algorithm

3.4.1 Self-correlation Function

The self-correlation function of signal $x(t)$, $R_x(\tau)$ is given as:

$$R_x(\tau) = E[(x(t)x(t+\tau))] = \lim_{T \rightarrow \infty} \frac{1}{T} \int_0^T x(t)x(t+\tau)dt \quad (6)$$

Self-correlation function describes a correlation degree of a single in the case of a time span τ .

3.4.2 Application of Self-correlation Function

Suppose a sinuous signal wave of frequency $\omega = 2\pi f$, magnitude A, initial phase ϕ is expressed by the following equation:

$$x(t) = A \sin(\omega t + \phi) \quad (7)$$

When $\tau = 0$, the self-correlation function of periodic signal $x(t)$ is expressed by:

$$R_x(0) = \frac{1}{T} \int_0^T x^2(t)dt = \frac{1}{T} \int_0^T (A \sin(\omega t + \phi))^2 dt = \frac{A^2}{2} \quad (8)$$

In this system, the discrete signal sequences after $x(t)$ is converted by ADC devices can be expressed as:

$$x_N(k) = A \sin(\omega k \Delta t + \phi) \quad (9)$$

where

$$\begin{aligned} \Delta t &: \text{Sampling interval.} \\ N &: \text{the no. of sampling points per period} \\ k &: \text{the sequence no. of the sampling points} \end{aligned}$$

When $\tau = 0$, the self-correlation function of discrete periodic signal $x_N(k)$ is given as:

$$R_x(0) = \frac{1}{N} \sum_{n=0}^{N-1} x^2(n) = \frac{A^2}{2} \quad (10)$$

Rearrange (8):

$$A = \sqrt{2 * \frac{1}{N} \sum_{n=0}^{N-1} x^2(n)} \quad (11)$$

According to the (9), the self-correlation function of discrete periodic signal sequence can be used to calculate the magnitude of the signal.

3.4.3 Correlation Function

The correlation function of signal waves $x(t)$ and $y(t)$, $R_{xy}(\tau)$, is given by the following:

$$R_{xy}(\tau) = E[x(t)y(t+\tau)] = \lim_{T \rightarrow \infty} \frac{1}{T} \int_0^T x(t)y(t+\tau)dt \quad (12)$$

Correlation function describes a correlation degree of two signals in the case of time span is τ .

3.4.4 Application of Correlation Function

Suppose a sinuous signal wave of frequency $\omega = 2\pi f$, magnitude A, initial phase ϕ is given by:

$$x(t) = A \sin(\omega t + \phi) \quad (13)$$

Suppose a second sinuous signal wave of frequency $\omega = 2\pi f$, magnitude B, initial phase θ is given as follows:

$$y(t) = B \sin(\omega t + \theta) \quad (14)$$

When $\tau = 0$, the correlation function of periodic signal $x(t)$ and $y(t)$ is given by the following:

$$R_{xy}(0) = \frac{1}{N} \sum_{k=0}^{N-1} x(k)y(k) = \frac{AB}{2} \cos(\phi - \theta) \quad (15)$$

When $\tau = 0$, the correlation function of two discrete signal sequences after $x(t)$ and $y(t)$ are converted by ADC devices can be expressed as follows:

$$R_{xy}(0) = \frac{1}{N} \sum_{k=0}^{N-1} x(k)y(k) = \frac{AB}{2} \cos(\phi - \theta) \quad (16)$$

where

$$\begin{aligned} N &: \text{the number of sampling points per period} \\ k &: \text{the sequence No. of the sampling points.} \end{aligned}$$

Rearrange (16) as follows:

$$\phi - \theta = \arccos\left(\frac{2}{NAB} \sum_{k=0}^{N-1} x(k)y(k)\right) = \arccos\left(\frac{2R_{xy}(0)}{AB}\right) \quad (17)$$

According to (17), the phase angle deviation of two periodic signal waves can be obtained if the correlation function value when $\tau = 0$ and two signal waves' magnitudes have been known.

3.5 Software Algorithm Procedure

The detail procedure of processing the data is as follows:

1. Sample the voltage signal and leakage current signal of MOA at the same time, and save the sampling data to RAM.
2. Filter the sampling data sequences of voltage signal and the total leakage current signal.
3. Obtain the period of signal wave through the Zero Crossing Technique.
4. Obtain the new data sequence through the interpolation algorithm.

5. Obtain the magnitude value of voltage and total leakage current using self-correlation algorithm and get the phase angle deviation of voltage and total leakage current using correlation algorithm.
6. Obtain the resistive current component of the leakage current of MOA.

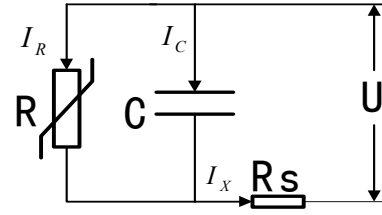


Fig.8 Circuit for experiment

4. Anti-interference Measures

In addition to the anti-interference measures in software, there are many anti-interference measures used in hardware. The printed circuit board is shielded by two metal boxes; double-twisted shield lines are used for signal measuring line. In this way, the electromagnetic interference has been effectively eliminated. In the input port of PT signal, analog active filter was used to eliminate the high frequency harmonic components. In the power supply, rechargeable battery was used as the power supply for the tester. Through these measures the interference on power supply was avoided.

5. Experimental Validation in the Laboratory

In order to validate the precision of the measure results of the tester, we proceed to perform actual experiments in laboratory.

The circuit of experiments is shown as Fig.8. In circuit the R is a rheostat with precision of 0.01%, C is a standard capacitance with precision of 0.0001 μ f, R_s is a sampling resistance between which the tester can fetch the I_x to system and U is provided by a INSTEK power source with the precision of 0.1%.

Table 1 shows the results of the measurement of the tester. It can be shown from the tested data that the maximum relative errors of the resistive component I_R in three groups are as follows:

$$\gamma_{I_{R1}} = \frac{0.001}{0.058} = 1.7\%,$$

$$\gamma_{I_{R2}} = \frac{0.001}{0.110} = 0.91\%,$$

$$\gamma_{I_{R3}} = \frac{0.002}{0.175} = 1.14\%;$$

To integrate the above, the relative error of the resistive component I_R can be known:

$$\gamma_{I_R} = \max(\gamma_{I_{R1}}, \gamma_{I_{R2}}, \gamma_{I_{R3}}) = 1.7\%$$

6. Conclusion

In the design of a tester for leakage current, a powerful floating point DSP is used. Some advanced software algorithms are embedded in DSP program using C language. The resultant tester has higher stability and has high anti-interference capability. According to the results of the measurement, it is proved that the tester for leakage current of MOA has achieved high precision in measuring resistive component of leakage current, which is important to judge the condition of the MOA. With the help of the tester, the operation conditions of MOA can be assessed or evaluated timely and correctly.

Table 1 Results of measurements

C=0.045uF R=500K Ω							
U (Volt)		I_x (mA)		I_R (Peak Value)(mA)		φ (Degree)	
Real	Measured	Real	Measured	Real	Measured	Real	Measured
62.00	62.06	0.896	0.896	0.058	0.058	87.30	87.21
62.00	62.02	0.896	0.895	0.058	0.059	87.30	87.25
62.00	61.95	0.896	0.894	0.058	0.059	87.30	87.24
C=0.045uF R=800K Ω							
U (Volt)		I_x (mA)		I_R (Peak Value)(mA)		φ (Degree)	
Real	Measured	Real	Measured	Real	Measured	Real	Measured
62.00	62.06	0.898	0.900	0.110	0.111	84.94	84.88
62.00	62.02	0.898	0.901	0.110	0.111	84.94	84.84
62.00	61.95	0.898	0.900	0.110	0.111	84.94	84.85
C=0.045uF R=1500K Ω							
U (Volt)		I_x (mA)		I_R (Peak Value)(mA)		φ (Degree)	
Real	Measured	Real	Measured	Real	Measured	Real	Measured
62.00	62.06	0.905	0.904	0.175	0.177	81.94	81.86
62.00	62.02	0.905	0.903	0.175	0.177	81.94	81.88
62.00	61.95	0.905	0.904	0.175	0.176	81.94	81.87

REFERENCES

- Akbar M., Ahamd M., 1999, "Failure Study of Metal-Oxide Surge Arresters", *Electric Power System Research* 50, pp 79-82.
- Lundquist J. et al., 1990, "New Method for Measurement of Resistive Leakage Currents of Metal-Oxide Surge Arresters In Service", *IEEE Transactions on Power Delivery*, Vol.5, No.4, November.
- Sun S.Q., 1998, "Fluctuations and Flickers of the Voltage of Power System," Beijing: Chinese Electric Publishing Company.
- Cai B., 1998, *The Frequency of Power System*, Beijing: Chinese Electric publishing company.
- Xu K.M., Xu Y., Liu F.P., 1991, "High Harmonic Waves Of the Power System," Chongqin Publishing Company Of Chongqin University.